Thermal Zero Drift Compensation of Pressure Sensor Based on Data Mining and BP Neural Network

Ya-ping Li(✉) and Dan Zhao

College of Mechatronic Engineering, Beijing Polytechnic, Beijing 100176, China

Abstract. Due to the poor compensation accuracy, the traditional compensation algorithm for thermal zero shift of pressure sensor results in large error of pressure measurement. Therefore, this paper proposes a pressure sensor thermal zero drift compensation algorithm based on data mining and BP neural network. Combined with the data mining process, the characteristics of the thermal zero drift of the pressure sensor are analyzed, and the hysteresis and nonlinear characteristic curve of the pressure sensor is obtained to prepare for the compensation of the thermal zero drift. Then BP neural network is introduced to determine the parameter update mode, which is effectively combined with artificial fish swarm algorithm, and the compensation of pressure sensor thermal zero shift is realized by implementing the thermal zero shift compensation algorithm of pressure sensor. The experimental results show that the pressure measurement error range of the algorithm in this paper is 0.30 N–1.45 N. Compared with the three existing algorithms, the pressure measurement error of the algorithm in this paper is smaller, which indirectly shows that the algorithm in this paper has a higher thermal zero drift compensation accuracy, which fully shows that the algorithm in this paper compensates better performance.

Keywords: Data mining · BP neural network · Pressure sensor · drift compensation · Artificial fish swarm algorithm

1 Introduction

The three foundations of modern information technology are information collection, transmission and processing technology, namely sensor technology, communication technology and computer technology, which constitute the "sense", "nerve" and "brain" of information technology system respectively. The most important component of information acquisition system is sensor, which is placed in the front of the system. In this case, sensor can be called cutting-edge technology [1]. With the development of communication technology and computer technology, sensor technology has been improved. Sensor is a kind of detection device, which can feel the measured information and transform the detected information into electrical signal or other required information output according to certain rules, so as to meet the requirements of information transmission,

S. Liu and X. Ma (Eds.): ADHIP 2021, LNICST 416, pp. 94–104, 2022.
https://doi.org/10.1007/978-3-030-94551-0_8

processing, storage, display, recording and control. Sensor is the first step to realize automatic detection and control.

The pressure sensor is one of the key types of sensors. The core of the pressure sensor is the diffused silicon resistance bridge, and the single chip microcomputer technology is used to collect data, process and output the display results. The piezoresistive coefficient of diffused silicon is a function of temperature, so there is a temperature drift of sensitivity. There are many factors that affect the temperature, such as the change of measuring environment, the change of measuring circuit heat, etc.

The zero point of pressure sensor has thermal drift, electrical drift and time drift [2, 3]. The thermal zero drift of pressure sensor will lead to the increase of temperature variation and the change of internal circuit parameters, which will lead to the output of interference signal which has nothing to do with the measurement and greatly affect the performance of pressure sensor. The existing thermal zero drift compensation algorithm of pressure sensor mainly includes bridge arm series and parallel constant resistance algorithm, bridge arm thermistor compensation algorithm and bridge external series and parallel thermistor compensation algorithm. Through investigation and research, it is found that the existing algorithms have the problem of large measurement pressure error.

Based on data mining and BP neural network, a new compensation algorithm for thermal zero drift of pressure sensor is designed in this paper to overcome the shortcomings of traditional compensation algorithms. The design idea of this method is as follows:

(1) Combined with the data mining process, the thermal zero drift characteristics of the pressure sensor were analyzed, and the hysteresis nonlinear characteristic curves of the pressure sensor were obtained to prepare for the thermal zero drift compensation.
(2) BP neural network was introduced to determine the parameter update mode, which was effectively combined with artificial fish swarm algorithm, and then the compensation of pressure sensor thermal zero shift was realized by implementing the thermal zero shift compensation algorithm of pressure sensor.
(3) Experimental verification shows that: compared with the three existing algorithms, the proposed algorithm has a smaller error in measuring pressure, which indirectly indicates that the proposed algorithm has a higher compensation accuracy for thermal zero drift.

2 Research on Compensation Algorithm for Thermal Zero Drift of Pressure Sensor

2.1 Analyze the Characteristics of the Thermal Zero Drift of the Pressure Sensor Through Data Mining

The so-called zero point output of the pressure sensor refers to the output of the pressure sensor when there is no external pressure under a certain reference temperature and a certain excitation source. The zero output voltage can sometimes be larger than the output voltage at full scale. At this time, a resistor can be connected in series or in parallel

with a certain bridge arm to make the bridge output zero, which is easy to achieve at a certain temperature [4]. The parameter to judge the quality of the zero point output of a pressure sensor is the ratio of the maximum zero point output to the upper range limit of the sensor. If the ratio is less than 0.8%, the zero point output of the sensor is considered to be small and can be ignored; if it is greater than 4%, the zero point output is equivalent big.

The main reasons for the zero-point output of the pressure sensor include: first, the difference between the design size of the force sensitive resistance bar and the actual size formed by lithography, and the inconsistency in the resistance value of the resistance bar due to the uneven doping concentration; Second, the stress introduced by the package is applied to the sensor to produce the output. Therefore, this study analyzes the characteristics of thermal zero drift of pressure sensors through data mining, and the process is as follows:

The relationship curve between the output voltage of the pressure sensor and the pressure is shown in Fig. 1.

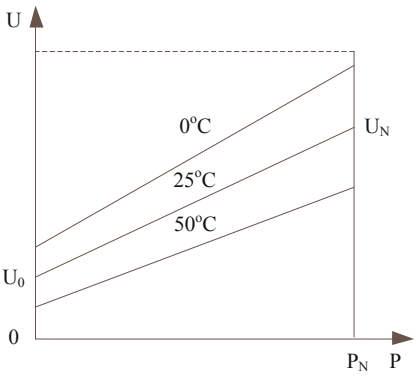

Fig. 1. Schematic diagram of relationship between output voltage and pressure of pressure sensor

In Fig. 1, U represents the output voltage of the pressure sensor; P represents the pressure value of the pressure sensor.

As shown in Fig. 1, it shows the relationship between the typical output voltage of the pressure sensor and the pressure under a certain excitation source. The three straight lines respectively represent the output conditions of the sensor at 0 °C, 25 °C and 50 °C. The zero point of the pressure sensor affected by temperature has changed significantly. This is because the doping of the force-sensitive resistor strips is inconsistent, resulting in a difference in the temperature coefficient of resistance. Considering only a single temperature situation, the zero-point output voltage offset can easily be offset by adjustment [5]. However, after the temperature changes, a new zero point output will appear. This phenomenon is called temperature drift of the zero point output voltage, or thermal zero point drift for short. When the three curves in Fig. 1 are subjected to the same initial pressure P_0, the output difference is caused by the thermal zero drift. Thermal zero drift is one of the important indicators of the performance of pressure sensors. Generally, the

thermal zero drift coefficient α_0 is used to represent:

$$\alpha_0 = \frac{U_0^{\max}(T) - U_0^{\min}(T_0)}{\Delta T\left[\overline{U}_F - \overline{U}_0\right]} \times 100\%FS/^{\circ}\mathrm{C} \tag{1}$$

In Eq. (1), $U_0^{\max}(T)$ is the maximum zero point output at a reference temperature T; $U_0^{\min}(T_0)$ is the minimum zero point output at a reference temperature T_0; ΔT is the temperature working range of the sensor; $\overline{U}_F$ is the average value of the full-scale output at each reference temperature; $\overline{U}_0$ is the average value of the zero point output at each reference temperature; FS is the unit name of the thermal zero point drift coefficient α_0.

Full scale output refers to the maximum effective output of the pressure sensor within the required range under the specified reference temperature and certain excitation current or voltage conditions [6]. As shown in Fig. 1, the full scale output is:

$$U_{sig}^{N}(T_0) = U_N(T_0) - U_0(T_0) \tag{2}$$

In formula (2), $U_{sig}^{N}(T_0)$ is the maximum effective output at a reference temperature T_0; $U_N(T_0)$ is the upper limit of the standard full scale at a reference temperature T_0; $U_0(T_0)$ is the zero point output value at a reference temperature T_0.

When the force-sensitive resistor is distributed in the appropriate area of the silicon diaphragm, the output signal will be the largest when under pressure, and the full scale should be widened as much as possible. The sensitivity is usually used to describe the performance of the pressure sensor. The sensitivity S is defined as:

$$S = \frac{1}{V_B}\frac{U_N - U_0}{P_N} = \frac{1}{V_B}\frac{U_{sig}^{N}}{P_N} \tag{3}$$

In formula (3), V_B is the external excitation voltage; P_N is the upper limit of the sensor range. It can be seen from the formula (3) that the full-scale output U_{sig}^{N} is equal to the sensitivity, V_B multiplied by the upper limit of the range, that is, the full-scale output is:

$$U_{sig}^{N} = S \times V_B \times P_N \tag{4}$$

Pressure sensitivity S and full-scale output U_{sig}^{N} both decrease with increasing temperature. This is because the pressure sensitivity is proportional to the piezoresistive coefficient, and the piezoresistive coefficient decreases with increasing temperature. In addition, the thermal stress is caused by the difference between the two sides of the force sensitive resistor $p-n$ junction and the thermal expansion coefficient of the surface SiO_2 or the passivation layer Si_3N_4, resulting in an additional piezoresistive effect, which is also related to temperature. The thermal sensitivity drift is also a measure of the quality of the pressure sensor. One of the important indicators [7]. The expression of thermal sensitivity drift coefficient K_0 is:

$$K_0 = \frac{\Delta U_F^{\max}(T) - \Delta U_F^{\min}(T_0)}{\left[\overline{U}_F - \overline{U}_0\right]\Delta T} \times 100\%FS/^{\circ}\mathrm{C} \tag{5}$$

In Eq. (5), $\Delta U_F^{\max}(T)$ refers to the maximum value of full-scale output minus zero output at a reference temperature T; $\Delta U_F^{\min}(T_0)$ refers to the minimum value of full-scale output minus zero output at a reference temperature T_0.

2.2 Analysis of Hysteresis and Nonlinear Characteristics of Pressure Sensors Through Data Mining

Based on the analysis results of the thermal zero drift characteristics of the pressure sensor, the hysteresis nonlinear characteristic curve of the pressure sensor is obtained through the data mining process, as shown in Fig. 2.

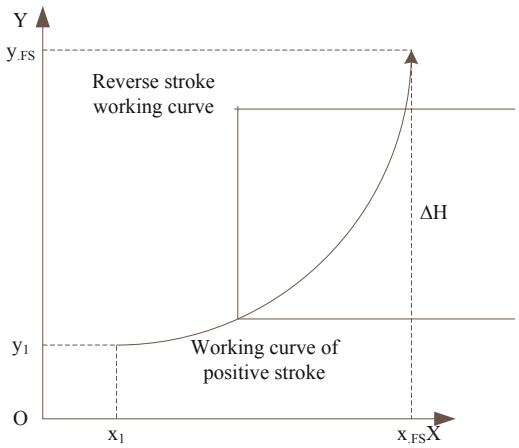

Fig. 2. Hysteresis and nonlinear characteristic curve of pressure sensor

As shown in Fig. 2, the hysteresis nonlinearity refers to the degree of inconsistency between the positive and negative stroke input and output curves of the sensor in the full range. The hysteresis nonlinear characteristics widely exist in sensors, piezoelectric ceramics, ferromagnets, semiconductor materials and smart materials, etc. field. As a pressure sensor with excellent performance, the pressure sensor also has hysteresis and nonlinear characteristics, which limits the accuracy of the measurement [8]. The magnitude of hysteresis nonlinearity can be determined by pressure calibration experiments. In the calibration experiment of the pressure sensor, first calculate the difference between the arithmetic mean of the forward output and the arithmetic mean of the reverse output at a set pressure measurement point:

$$\Delta y_{H_i} = \overline{y}_{+i} - \overline{y}_{-i} (i = 1, 2, 3, \cdots) \tag{6}$$

In Eq. (6), $\overline{y}_{+i}$ and $\overline{y}_{-i}$ refer to the arithmetic mean value of forward output and backward output respectively; the value range of i is $(1, +\infty)$.

The calculation formula of sensor hysteresis is:

$$\xi_H = \frac{|\Delta y_H|}{y_{FS}} \times 100\% \tag{7}$$

In formula (7), ξ_H is the hysteresis value of the sensor; y_{FS} is the full-scale output.

Solve the hysteresis and nonlinear problems of pressure sensors. Generally, data fusion algorithms are used to compensate. The pressure sensor designed in this research

uses the BP neural network algorithm to compensate for the hysteresis. Formula (7) is used to calculate the change in the hysteresis of the sensor before and after compensation to verify the effect of the hysteresis correction.

2.3 BP Neural Network Algorithm Introduction

BP neural network algorithm is a multilayer feedforward network trained by error back propagation algorithm, which is usually used for data classification and prediction. The most important part of BP neural network algorithm is the learning part of its weight and threshold. Generally, the learning process is divided into two parts. One part is the forward transmission process, that is, the input samples are transferred from the input layer, and then processed layer by layer by each hidden layer, and then transferred to the output layer. The other part is the process of error reverse transmission, that is, if the actual output of the output layer is not the same as the expected output, the error is used as the adjustment signal to reverse the transmission layer by layer, and the connection weight matrix between neurons is processed to reduce the error. After repeated learning process, the error is finally reduced within the initial set range [9].

BP neural network is composed of input layer, output layer and intermediate layer between them. The middle layer can be single-layer or multi-layer. Because the middle layer is not connected with the external environment, it is also called hidden layer. The input layer, hidden layer and output layer are connected with each other, but the nodes of single layer are not connected. The structure of BP neural network is shown in Fig. 3.

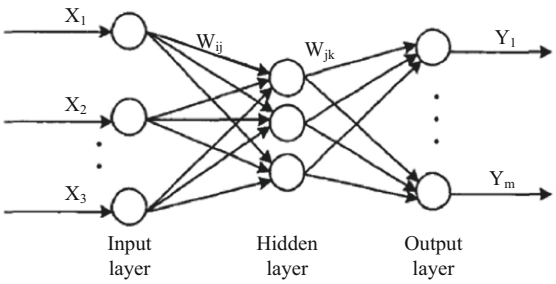

Fig. 3. BP neural network structure diagram

It can be seen from Fig. 3 that the BP neural network algorithm is composed of multiple input layers, hidden layers and output layers. Specifically, the input layer accepts external input by a series of input signals from X_1 to X_2. Correspondingly, the output layer is composed of a series of network output values, which is $Y_1, Y_2, \cdots, Y_m$ in the figure above. The hidden layer between the two is represented by the corresponding network weights W_{ij} and W_{jk}. In addition, θ_j and θ_k can be used to represent the network threshold between two adjacent layers. Then the output of each node can be obtained by

the following formula:

$$\begin{cases} x_j^* = f\left(\sum_{i=1}^{n} w_{ij} x_j - \theta_j\right) \\ y_k = f\left(\sum_{j=1}^{l} w_{jk} x_j^* - \theta_k\right) \end{cases} \tag{8}$$

In Eq. (8), f represents the function transformation relationship between the input and output of neurons, which is called the excitation function and type S function:

$$f(x) = \frac{1}{1 + e^{-x}} \tag{9}$$

The prediction error E of BP neural network can be obtained, where o_k is the expected value of BP neural network:

$$E = \frac{1}{2} \sum_{k=1}^{m} (o_k - y_k) \tag{10}$$

If the error at this time is less than the previously set error, the calculation ends, otherwise it enters the error reverse transmission part.

Minute. In order to further reduce the error, the gradient descent method is used to adjust and update the weights and thresholds. The so-called gradient descent method is to adjust the weights and thresholds to the negative gradient direction, so that the adjustment amount of the two and the gradient of the error fall into direct ratio. The parameter adjustment formula is:

$$\begin{cases} W'_{ij} = w_{ij} - \eta \frac{\partial E}{\partial w_{ij}} \\ W'_{jk} = w_{jk} - \eta \frac{\partial E}{\partial w_{jk}} \\ \theta'_j = \theta_j - \eta \frac{\partial E}{\partial \theta_j} \\ \theta'_k = \theta_k - \eta \frac{\partial E}{\partial \theta_k} \end{cases} \tag{11}$$

In formula (11), η represents the learning rate, and the value range is [0, 1]. Train the BP neural network according to the result of formula (11). If the error is less than the set error, the learning ends, otherwise it will enter the next round of learning.

2.4 Design of Thermal Zero Drift Compensation Algorithm

Based on the above introduced BP neural network algorithm combined with artificial fish school algorithm, a pressure sensor thermal zero drift compensation algorithm is introduced.

Since the artificial fish school algorithm can iteratively optimize in the global scope, combining the artificial fish school algorithm with the BP neural network can combine the advantages of the two to make up for its own shortcomings. In other words, the artificial fish swarm algorithm can be used for global optimization to solve the problem of BP neural network being easily trapped in local minimums [10, 11]. Assuming that

each artificial fish in the artificial fish school represents a BP neural network, the initial weights and thresholds of the BP neural network need to be optimized to correspond to the individual state of the artificial fish, and the best position of the BP neural network is obtained by finding the optimal artificial fish position. Optimal weights and thresholds, and then use the obtained optimal weights and thresholds to train the BP neural network. This study defines the fitness function F of the artificial fish school as the reciprocal of the mean square error value E of the BP neural network output result and the expected value result.

The specific steps of the pressure sensor thermal zero drift compensation algorithm are as follows:

Step 7: if *num* reaches the maximum number of iterations *trynumber* or the error of the solution is less than the set minimum error ε, the behavior ends and the calculation result is output, otherwise $num = num + 1$, go to step 4.

Through the above process, the thermal zero drift compensation of pressure sensor is realized, which provides effective means for the application and development of pressure sensor.

3 Simulation Experiment and Result Analysis

The above process realizes the design of thermal zero drift compensation algorithm of pressure sensor based on data mining and BP neural network, but whether it can solve the problems of existing algorithms is uncertain. Therefore, MATLAB software is used to design simulation experiments to verify the compensation performance of the proposed algorithm.

3.1 Simulation Experiment Data Acquisition and Experiment Preparation

The experiment of the temperature influence of the pressure sensor is carried out in an experiment box. The equipment used in the experiment is: two pressure sensors, a thermostat, a signal simulator, and a standard thermometer.

During the measurement, it needs to wait for the pressure value at each set temperature point before reading, and it needs to carry out 10 repeated experiments and read 10 times of data, and then it needs to average the 10 times of data corresponding to each observation point, so as to complete the acquisition of the measured value of the pressure sensor. For the calculation of the standard value of the pressure sensor, it is necessary to make further correction on the basis of the measured value of the pressure sensor, that is, to add the corresponding correction value on the basis of the average value of each test point. Some of the data are shown in Table 1.

The difference between the measured value of the pressure sensor and the standard value is taken as the measurement error value of the pressure sensor, the temperature value is taken as the abscissa, and the measurement error value is taken as the ordinate.

The temperature influence error curve of the pressure sensor corresponding to each temperature is drawn, as shown in Fig. 4. Based on the data in Fig. 4, BP neural network algorithm was trained to prepare for the simulation experiment.

Table 1. Part of simulation experiment data table

Interference amount (°C)	Measured value	Standard value	Error
20	23.08	23.55	0.47
25	22.57	25.05	2.48
30	45.89	48.25	2.36
35	45.59	48.00	2.41
40	68.65	71.20	2.55
45	67.65	71.25	3.60
50	88.77	90.35	1.58
55	85.40	92.30	6.90
60	92.50	96.50	4.00
65	91.88	97.60	5.72

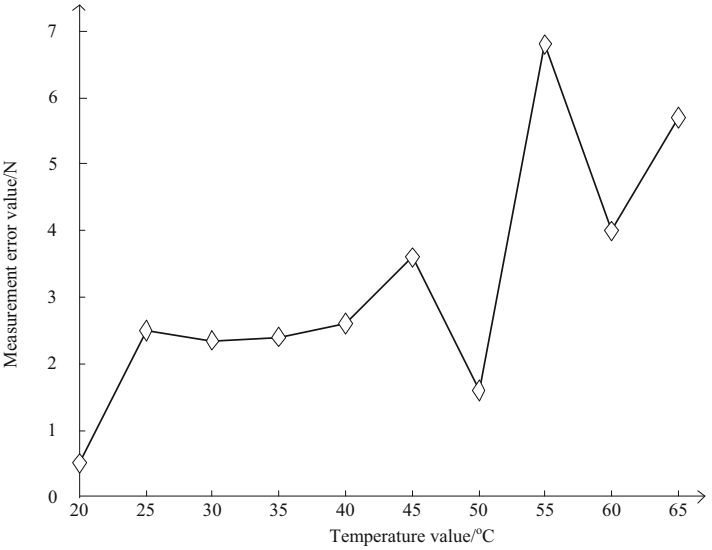

Fig. 4. Temperature influence error curve of pressure sensor

3.2 Analysis of Results

In order to clearly show the performance of the proposed algorithm, the bridge arm series and parallel appropriate constant resistance algorithm, the bridge arm thermistor compensation algorithm and the bridge outside series and parallel thermistor compensation algorithm and the proposed algorithm are used for simulation and comparative experiments. In order to facilitate the experiment, the above existing algorithms are

called existing algorithm 1, existing algorithm 2 and existing algorithm 3, and the measurement pressure error is obvious after compensation It shows the performance of the algorithm.

The measured pressure error data obtained by simulation experiment is shown in Table 2.

Table 2. Data sheet of measurement pressure error

Interference amount (°C)	Measurement pressure error/N			
	The algorithm in this paper	Existing algorithm 1	Existing algorithm 2	Existing algorithm 3
20	0.30	2.13	2.56	2.48
25	1.23	2.00	2.01	2.44
30	1.20	2.10	3.10	2.69
35	1.11	2.11	3.00	2.58
40	1.01	2.05	2.99	2.15
45	1.00	2.56	2.01	2.12
50	1.03	2.48	2.55	2.30
55	1.22	2.55	2.41	3.10
60	1.45	2.97	3.01	3.00
65	0.98	3.01	3.12	3.05

According to the data in Table 2, the measurement error range of the existing algorithm 1 is 2.00–3.01; the measurement error range of the existing algorithm 2 is 2.01–3.12; the measurement error range of the existing algorithm 3 is 2.12–3.10; the measurement error range of the proposed algorithm is 0.30–1.45. Through the comparative study, it is found that the pressure measurement error of the proposed algorithm is far lower than the existing three algorithms.

The reasons for the above results are as follows: compared with the existing three algorithms, the proposed algorithm has smaller pressure measurement error, which indirectly indicates that the proposed algorithm has higher accuracy of thermal zero drift compensation, and fully indicates that the proposed algorithm has better compensation performance. The reason for the above results is that the algorithm in this paper combines the data mining process to analyze the thermal zero drift characteristics of the pressure sensor and obtain the hysteresis nonlinear characteristic curve of the pressure sensor, which makes sufficient preparation for the thermal zero drift compensation. Then, BP neural network is introduced to determine the parameter updating mode, which is combined with artificial fish swarm algorithm effectively, thus improving the accuracy of thermal zero drift compensation.

4 Conclusion

In this paper, data mining and BP neural network are applied to the process of pressure sensor thermal zero drift compensation, which greatly improves the accuracy of pressure sensor thermal zero drift compensation, reduces the pressure sensor measurement error, and provides a certain reference value for the research of pressure sensor thermal zero drift compensation. Although the existing experimental results can prove the effectiveness of the proposed algorithm, the explanability of the obtained experimental results is low due to the lack of experimental data in the simulation experiment, and there are also certain deviations. Therefore, in the following research, the compensation algorithm of thermal zero shift of pressure sensor will be further studied and discussed, the amount of simulation data will be increased, and the compensation results will be optimized.

Fund Projects. Research on temperature compensation method of silicon sapphire high temperature pressure sensor (CJGX2016-KY-YZK032).

References

1. Zhang, J., Soangra, R., Lockhart, T.: Automatic detection of dynamic and static activities of the older adults using a wearable sensor and support vector machines. Sci **2**(3), 56 (2020)
2. Song, H., Chen, W., Wang, X., et al.: Detection of methanol by a sensor based on rare-earth doped TiO 2 nanoparticles. J. Wuhan Univ. Technol.-Mater. Sci. Ed. **33**(5), 1070–1075 (2018)
3. Utama, D.T., Lee, S.G., Baek, K.H., et al.: Effects of high-pressure processing on taste-related ATP breakdown compounds and aroma volatiles in grass-fed beef during vacuum aging. Asian-Australas. J. Anim. Sci. **31**(8), 1336–1344 (2018)
4. Ogura, Y., Sato, K., Miyahara, S.I., et al.: Efficient ammonia synthesis over a Ru/La0.5Ce0.5O1.75 catalyst pre-reduced at high temperature. Chem. Sci. **9**(8), 2230–2237 (2018)
5. Zanos, T.P., Silverman, H.A., Levy, T., et al.: Identification of cytokine-specific sensory neural signals by decoding murine vagus nerve activity. Proc. Natl. Acad. Sci. U.S.A. **115**(21), 4843–4852 (2018)
6. Gao, X., Li, H., Wei, J.X.: MiR-4421 regulates the progression of preeclampsia by regulating CYP11B2. Eur. Rev. Med. Pharmacol. Sci. **22**(6), 1533–1540 (2018)
7. Bakis, A., Isik, E., El, A., Ülker, M.: Mechanical properties of reactive powder concretes produced using pumice powder. J. Wuhan Univ. Technol.-Mater. Sci. Ed. **34**(2), 353–360 (2019). https://doi.org/10.1007/s11595-019-2059-1
8. Liu, S., Lu, M., Li, H., et al.: Prediction of gene expression patterns with generalized linear regression model. Front. Genet. **10**, 120 (2019)
9. Liu, S., Bai, W., Zeng, N., et al.: A fast fractal based compression for MRI images. IEEE Access **7**, 62412–62420 (2019)
10. Liu, S., Liu, D., Srivastava, G., Połap, D., Woźniak, M.: Overview and methods of correlation filter algorithms in object tracking. Complex Intell. Syst. **7**(4), 1895–1917 (2020). https://doi.org/10.1007/s40747-020-00161-4
11. Wu, Q., Zhang, C., Zhang, M., et al.: A modified comprehensive learning particle swarm optimizer and its application in cylindricity error evaluation problem. Int. J. Performability Eng. **15**(3), 2553 (2019)